https://doi.org/10.5194/egusphere-2026-1492
Preprint. Discussion started: 10 April 2026

The 2020 abrupt drainage of Jinwuco triggered lake- to land- terminus transition and lagged slowdown of Jinwu Glacier, southeastern Tibet

Yunyi Luo[1,2], Qiao Liu[1], Yin Fu[1], Xueyuan Lu[1,2], Yongsheng Yin[1,2], Jiawei Yang[1,2], Guoxiong Zheng[3], Xuyang Lu[1]

1 Key Laboratory of Mountain Hazards and Engineering Resilience, Institute of Mountain Hazard and Environment, Chinese Academy of Sciences, Chengdu 610213, China.

2 University of Chinese Academy of Sciences, Beijing 100049, China.

3 School of Earth and Environmental Sciences, Lanzhou University, Lanzhou 730000, People's Republic of China

Correspondence: Qiao Liu; liuqiao@imde.ac.cn

Abstract. Glacier–proglacial lake interactions can accelerate terminus retreat and dynamic thinning of lake-terminating glaciers. However, glacier responses to abrupt lake disconnection following glacial lake outburst floods (GLOFs) remain poorly quantified. Here, we investigate changes in surface velocity (2017-2025) and elevation (2002-2025) of Jinwu Glacier (southeast Tibet, China), whose proglacial lake (Jinwuco) drained during a GLOF on 26 June 2020, shifting the glacier from lake- to land-terminating conditions. Rapid lake drainage triggered a pronounced but lagged dynamic response. Ice-flow velocities within 0-200 m of the terminus decreased by ~49%, from ~40 m a^{-1} (2017-2020) to ~20 m a^{-1} (2022-2025). In contrast, velocity reductions in the upstream reach (600-1550 m) were smaller (~14%). Surface elevation thinning in the terminal 0-550 m section intensified from −2.90 m a^{-1} during 2002–2014 to −3.71 m a^{-1} during 2014–2025, whereas surface lowering in the 600-1550 m section slowed from −1.17 to −0.87 m a^{-1}, with a slight surface elevation increase in the topographic transition zone (500–750 m). Following the GLOF, the glacier terminus underwent slight advance and localized ice calving. These patterns suggest a short-lived longitudinal extension at the glacier terminus, followed by a shift toward a more compressive regime in the 500–750 m zone as downstream ice-flux demand weakened. This study provides the first quantitative evidence of glacier dynamic adjustment following a GLOF driven transition from lake- to land-terminating conditions.

https://doi.org/10.5194/egusphere-2026-1492
Preprint. Discussion started: 10 April 2026

1 Introduction

Since the 20th century, glaciers in most regions have retreated and thinned, and mass loss has accelerated over recent decades under continued global warming (Zemp et al., 2025; Hugonnet et al., 2021; Maurer et al., 2019). Glacier retreat promotes the formation and expansion of glacial lakes, driving rapid increases in both lake number and area (Wang et al., 2020; Shugar et al., 2020; Zhang et al., 2024). This development has increased the hazard and risk associated with glacial lake outburst floods (GLOFs) (Zhang et al., 2025; Zhang et al., 2023b; Zheng et al., 2021c). The sudden and catastrophic release of lake water during GLOFs can produce severe socio-economic and geomorphic impacts far downstream, threatening critical infrastructure such as hydropower facilities, bridges, and roads (Richardson and Reynolds, 2000). This problem is particularly acute in High Mountain Asia (HMA), where several high-magnitude GLOFs have been documented and glacial lakes continue to expand (Zheng et al., 2021a; Lützow et al., 2023; Zhang et al., 2025). Many studies have assessed GLOF hazard and risk at regional and local scales (Zhang et al., 2023b; Zheng et al., 2021c; Ahmed, 2025), with a primary focus on downstream process chains and impacts. In contrast, the role of GLOFs as event-driven perturbations to upstream source glaciers remains poorly quantified, particularly for glaciers in contact with proglacial lakes.

Proglacial lakes typically form through two main pathways. One involves the coalescence of multiple supraglacial ponds near the glacier terminus (Carrivick and Tweed, 2013). The other occurs when a retreating glacier exposes deeply carved subglacial depressions that progressively store water as retreat continues (Schomacker, 2010). Proglacial lakes can enhance glacier mass loss by promoting thermal undercutting and calving at the glacier terminus (Watson et al., 2020). Lake water also exerts buoyant support on the ice and reduces effective pressure, thereby lowering basal friction and increasing ice flow (Benn et al., 2007). Lake-terminating glaciers often behave differently from land-terminating glaciers. Several studies report faster flow and stronger velocity variability for lake-terminating glaciers (Pronk et al., 2021; Liu et al., 2020; King et al., 2018), as well as more pronounced mass loss near the terminus (Tsutaki et al., 2019; Maurer et al., 2019). Importantly, glacier–lake contact is not constant (Luo et al., 2025). Lake expansion and changes in terminus geometry can lead to progressive detachment from the lake. In contrast, GLOFs can lower the lake level abruptly, shifting glaciers from lake-terminating to land-terminating conditions. Unlike gradual detachment during long-term retreat, GLOF-driven

https://doi.org/10.5194/egusphere-2026-1492
Preprint. Discussion started: 10 April 2026

detachment represents a short-lived but strong perturbation, yet the magnitude and temporal evolution of the glacier dynamic response remain poorly understood. A recent study reported a dynamic response after the risk-mitigation lowering of a proglacial lake by 5 m at Longbasaba Glacier. The glacier accelerated above its mean flow speed, followed by a period of deceleration (Liu et al., 2020). This suggests that abrupt changes in terminus boundary conditions can induce strong short-term dynamic adjustments. Climate projections indicate a trend toward warmer and wetter conditions in monsoon-influenced parts of High Mountain Asia (HMA) (Kitoh, 2017; Sanjay et al., 2017), alongside an expected increase in GLOF occurrence (Zheng et al., 2021c). It is therefore important to quantify how GLOFs affect glacier termini and to characterize the subsequent short-term adjustment and longer-term evolution. Improved understanding of these processes is critical for constraining projections of glacier response and informing hazard assessment and risk management.

This study focuses on the Jinwuco–Jinwu Glacier system in southeastern Tibet, China. On 26 June 2020, the proglacial lake Jinwuco produced a GLOF during a period of high air temperature and heavy rainfall (Zheng et al., 2021b). The event caused a rapid lake-level decline and shifted Jinwu Glacier to a land-terminating glacier. We integrate multi-source historical remote-sensing data to reconstruct changes in terminus geometry, surface velocity, and surface elevation before and after the event. We then quantify how the GLOF driven step change in terminus boundary conditions affected glacier dynamics. Finally, we discuss the short-term response, potential lags, and the subsequent adjustment toward a new dynamic state.

2 Study area

Jinwu Glacier (30.335° N, 93.634° E) is located in the middle-upper Nidou Zangbo Basin in the eastern Nyainqentanglha, Tibetan Plateau (Fig. 1a, b). The glacier lies on the northern flank of Nenang Peak, the highest summit in the basin (Fig. 1c). The Nidou Zangbo basin covers ~1268 km² (Lehner and Grill, 2013) and spans an elevation range of ~3666 m a.s.l. based on the SRTM DEM. Basin topography is higher in the west and lower in the east, and the mean elevation exceeds 5000 m a.s.l. Most peaks rise above 6000 m a.s.l., with Nenang Peak reaching 6870 m a.s.l. Owing to this high relief setting, glaciers and glacial lakes are widespread. The basin contains 343 glaciers with a total area of ~385 km² (RGI 7.0). In 2018, 39 glacial lakes were mapped with a total area of ~3.0 km² (Wang et al., 2020). The regional

https://doi.org/10.5194/egusphere-2026-1492
Preprint. Discussion started: 10 April 2026

climate is strongly influenced by the monsoon, with cold winters and cool summers (Yao et al., 2012). Annual mean air temperature increased significantly during 1990–2025, with a linear warming rate of ~0.03 °C a^{-1} ($p = 0.01$, $R^2 = 0.16$; Fig. 1d). Jinwu Glacier is oriented approximately north to south and covers ~ 8.16 km^2 in 2025. Its lower tongue is partly debris covered and includes a pronounced icefall. The icefall has an elevation drop of ~300 m, and the maximum slope exceeds 35°, based on the SRTM DEM (Fig. 1e).

A moraine-dammed proglacial lake, Jinwuco, is located at the glacier terminus. Jinwuco produced a GLOF on 26 June 2020. The event was triggered by a large debris landslide from the western lateral moraine that entered the lake (Zheng et al., 2021b). Before the flood, the glacier tongue was in direct contact with the lake. The lake area was ~0.58 km^2 and its straight-line length was ~1.8 km, making it the largest glacial lake in the basin. After the outburst, the lake area rapidly decreased to ~0.27 km^2 in 2020, and lake level lowering led to loss of contact between the lake and the glacier terminus.

https://doi.org/10.5194/egusphere-2026-1492
Preprint. Discussion started: 10 April 2026

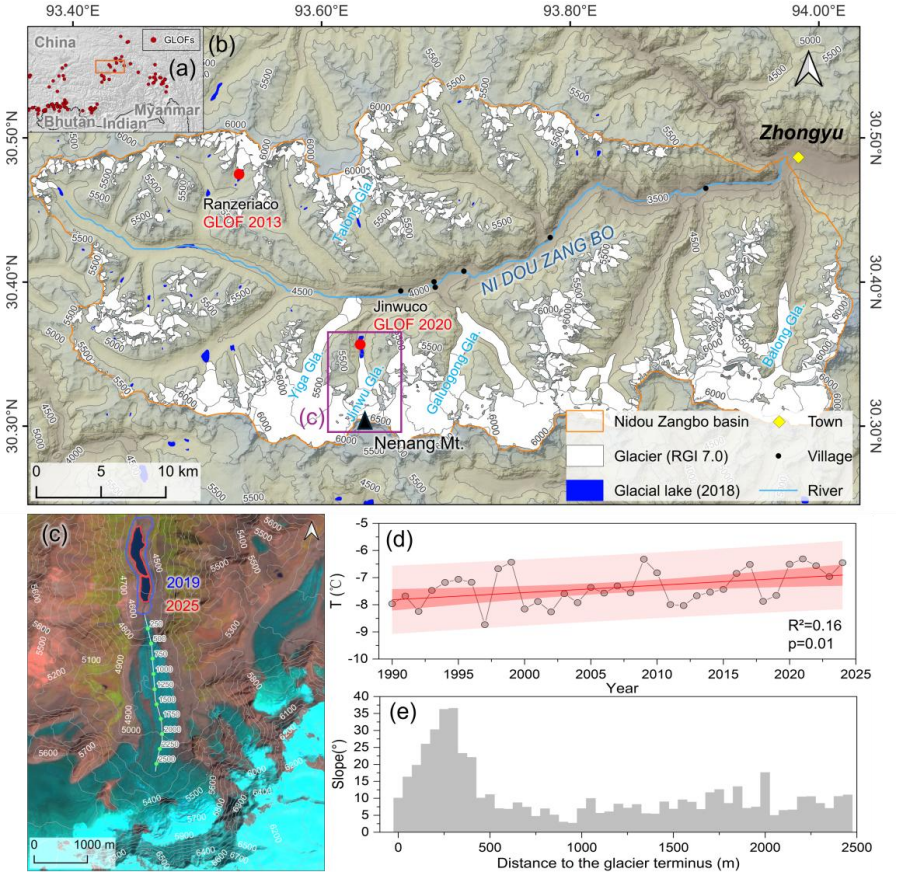

Figure 1 Study area and basic geographic setting of Jinwu Glacier in southeastern Tibet. (a) Distribution of reported glacial lake outburst floods (GLOFs) in southeastern Tibet (Lützow et al., 2023) and the location of the Nidou Zangbo basin. The basemap in panel (a) is Esri World_Shaded_Relief (Powered by Esri). (b) Overview map of the Nidou Zangbo basin showing glaciers (RGI 7.0), glacial lakes (Wang et al., 2020), rivers, and settlements, with Jinwuco and the 2020 GLOF site indicated. The hillshade in panel (b) is based on the SRTM DEM. (c) Sentinel-2 optical image acquired on 25 August 2024, with a close-up view of Jinwu Glacier and its proglacial lake (Jinwuco). (d) Interannual variability and linear trend in basin-mean annual air temperature from ERA5 during 1990–2025. (e) Longitudinal slope profile derived from the SRTM DEM along the main flowline of Jinwu Glacier as a function of distance from the glacier terminus. All numbers shown in the figure without explicit units are in meters (m).

3 Data and Methods

3.1 Glacial lake mapping

We reconstructed changes in the extent of Jinwuco from 1990 to 2025 based on historical remote sensing imagery (Table S1) using manual visual interpretation. Landsat imagery (TM/ETM+/OLI, 30 m

https://doi.org/10.5194/egusphere-2026-1492
Preprint. Discussion started: 10 April 2026

resolution) was used for the period from 1990 to 2015, and PlanetScope images (3 m resolution) were used for 2016 to 2025. The area uncertainty associated with lake-boundary delineation from optical imagery primarily depends on image quality and can be approximated as ±0.5 pixel (Salerno et al., 2012). In addition, the uncertainty introduced by manual delineation can be assumed to follow a Gaussian distribution (Hanshaw and Bookhagen, 2014). We estimated the uncertainty (δ) in glacial lake area using Eq.(1) (Hanshaw and Bookhagen, 2014)：

$$\delta = \frac{P}{G} \times \frac{G^2}{2} \times 0.6872 \quad (1)$$

where P is the perimeter of the glacial lake (m), G is the spatial resolution of the images used (m), 0.6872 is the revised coefficient under 1σ (i.e. approximately 69% of peripheral pixels are subjected to errors).

3.2 Surface velocity

We used 10 PlanetScope images (Table S1) to derive annual surface velocity fields for Jinwu Glacier from 2017 to 2025. To capture displacement over a full calendar year, we prioritized image pairs acquired in the second half of each year. In autumn and winter, terrain shadows often obscure large parts of the lower glacier (Fig. S1), reducing image texture and degrading feature tracking. We therefore mainly selected scenes from September and October to minimize shadow effects. We also prioritized images with minimal cloud and snow cover to improve tracking reliability and spatial coverage.

Surface velocities of Jinwu Glacier were derived using the Coregistration of Optically Sensed Images and Correlation (COSI-Corr) technique implemented in ENVI (Leprince et al., 2007). This approach has been widely applied to glacier motion monitoring and has shown robust performance (Gao et al., 2025; Li et al., 2023; Singh Jasrotia et al., 2024). We used a correlation window of 150 × 150 m (50 × 50 pixels) with a step size of 30 × 30 m (10 × 10 pixels). The search range was set to 90 × 90 m (30 × 30 pixels). Systematic biases in the east–west and north–south displacement components were corrected using stable terrain. Stable terrain was defined as non-glacier surfaces unaffected by clouds, lakes, or topographic shadows, and was further restricted to pixels with slopes <30°. To suppress outliers, we excluded pixels with velocities exceeding four times the normalized median absolute deviation (NMAD) (Fig. S2). Glacier velocity (GV) was then calculated using Eq. (2) and Eq. (3):

$$D = \sqrt{{V_x}^2 + {V_y}^2} \quad (2)$$

https://doi.org/10.5194/egusphere-2026-1492
Preprint. Discussion started: 10 April 2026

$$GV = \frac{D \times N}{A} \quad (3)$$

where D is the displacement measured between each image pair, V_x and V_y are the east–west and north–south displacement components, respectively, N is the time interval between the image pairs (days), and A is the number of days per year. To further improve robustness, we retained only velocity pixels with a signal-to-noise ratio (SNR) > 0.7. We assessed velocity uncertainty using residual displacements over stable, non-glacier terrain (Mattea et al., 2025; Paul et al., 2022). The mean residual displacement over stable terrain was 2.65 m a^{-1}. NMAD values ranged from 0.82 to 2.58 m a^{-1} (Table S1). We additionally used the open-access global glacier surface velocity dataset ITS_LIVE (1986–2022, 120 m resolution) as a benchmark for comparison (Gardner et al., 2025).

3.3 Surface elevation change

The DEMs used in this study were generated from ASTER L1A stereo data using the NASA Ames Stereo Pipeline (ASP) (Beyer et al., 2018). This approach has been widely applied to glacier surface elevation measurements (Brun et al., 2017; Bhattacharya et al., 2021). We produced three DEMs for the study area, dated 2 October 2002, 1 November 2014, and 13 June 2025. Surface elevation change was derived by DEM differencing. DEM biases may arise from limitations in DEM generation and from differences in processing strategies across datasets (Ke et al., 2020). To reduce these biases, we co-registered DEMs from different epochs following Nuth and Kääb (2011) and then removed the residual median vertical offset over stable terrain (Fig. S3). Stable terrain was defined as pixels with slopes below 30° and absolute elevation differences smaller than four times the NMAD (Mattea et al., 2025). Pixels with absolute elevation differences larger than 150 m were excluded (Hugonnet et al., 2021).

We quantified the systematic bias and random errors of DEM differencing using stable, non-glacier areas. For 2002–2014, the mean elevation difference over stable terrain was 0.05 m and the NMAD was 5.66 m. For 2014–2025, the mean elevation difference was −1.68 m and the NMAD was 6.46 m. We also used two open-access glacier surface elevation change datasets that cover the study area as independent references, spanning 2000–2019 (Hugonnet et al., 2021) and 2000–2016 (Brun et al., 2017).

https://doi.org/10.5194/egusphere-2026-1492
Preprint. Discussion started: 10 April 2026

4 Results

4.1 Long term evolution of Jinwuco

Since 1990, Jinwuco has undergone sustained expansion, followed by an abrupt decrease after the June 2020 GLOF (Fig. 2). The lake area was 0.371 ± 0.004 km² in 1990 and increased steadily to a maximum of 0.577 ± 0.004 km² in 2019, representing an increase of 0.206 km² (approximately +56%) relative to 1990 (Fig. 3). Over 1990–2019, the mean expansion rate was 6.51 × 10^{-3} km² a^{-1}. Following the 2020 GLOF, the lake area decreased sharply from 0.577 ± 0.004 km² in 2019 to 0.272 ± 0.004 km² in 2020, a reduction of 0.305 km² (approximately −53%). During 2020–2025, the lake area remained relatively stable at 0.25–0.27 km² (0.251 ± 0.004 km² in 2025).

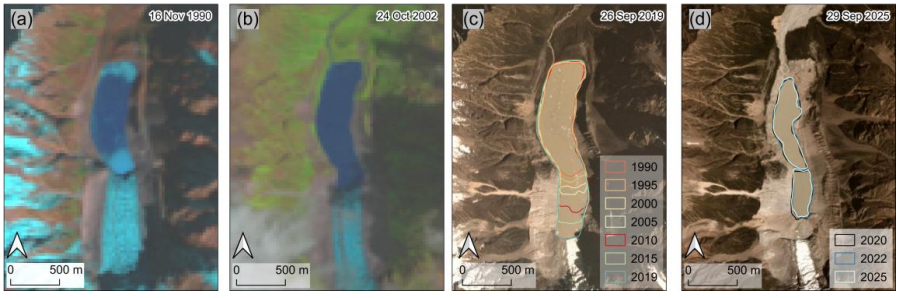

Figure 2 Multi-temporal evolution of the proglacial lake Jinwuco. (a–b) Landsat TM imagery as the basemap; (c–d) PlanetScope imagery as the basemap. Colored outlines denote lake extents (shorelines) mapped for different years.

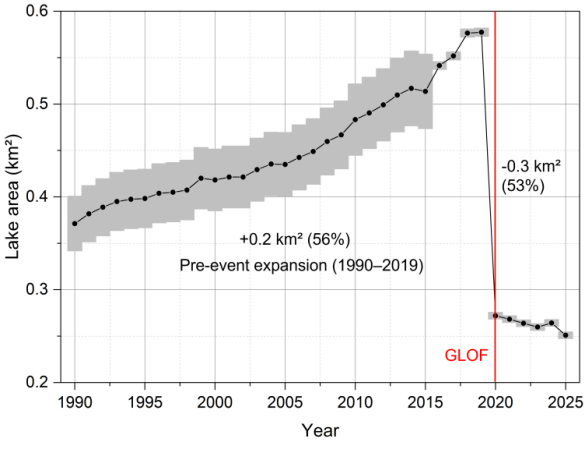

Figure 3 Lake area changes of Jinwuco during 1990–2025. Black dots denote the mapped lake area for each year. The grey shading indicates the uncertainty of lake area and the uncertainty calculation is described in Sect. 3.1.

https://doi.org/10.5194/egusphere-2026-1492
Preprint. Discussion started: 10 April 2026

4.2 Surface velocity

Following the June 2020 GLOF, the near-terminus flow regime transitioned to relatively low velocities. However, the dynamic response was clearly lagged, with the main deceleration emerging after 2021 and subsequently stabilizing (Fig. 4a,b). Specifically, within 0–200 m distance of the glacier terminus, mean ice-flow velocities were 41.82 ± 7.63 m a^{-1}, but decreased markedly to 21.28 ± 7.48 m a^{-1} (~49%) in 2022–2025 (Fig. 4c). In parallel, PlanetScope imagery during 2020–2021 indicates that the ice-cliff morphology progressively degraded, while the terminus position showed a slight advance (Fig. 5). In the upstream 600–1550 m section (Fig. 4d), the mean velocity also decreased from 38.25 ± 9.12 m a^{-1} during 2017–2021 to 32.87 ± 8.37 m a^{-1} during 2022–2025, representing a 14% reduction. Over the longer term, ITS_LIVE suggests an overall deceleration of Jinwu Glacier since 2000 (Fig. 4c, d), although the magnitude of deceleration in the downstream 0–200 m zone differs between ITS_LIVE and our measurements. These discrepancies are further discussed in Sect. 5.2.

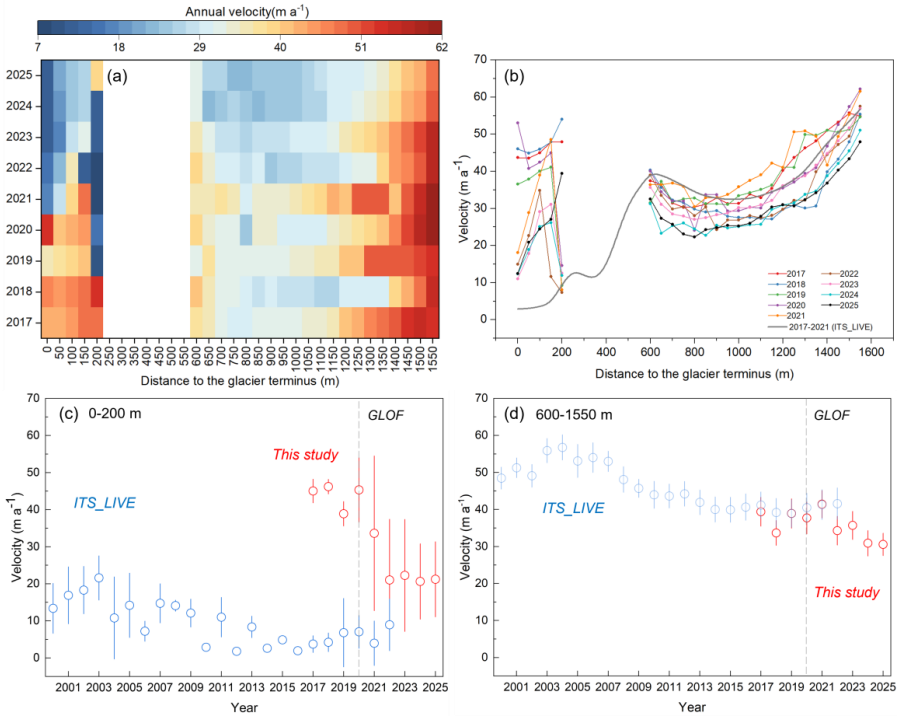

Figure 4 (a-b) Longitudinal profile of surface ice velocity along the center flowline (50m bin). Interannual variability in the mean surface velocity within 0–200 m (c) and 600-1550 m (d) from the glacier terminus.

https://doi.org/10.5194/egusphere-2026-1492
Preprint. Discussion started: 10 April 2026

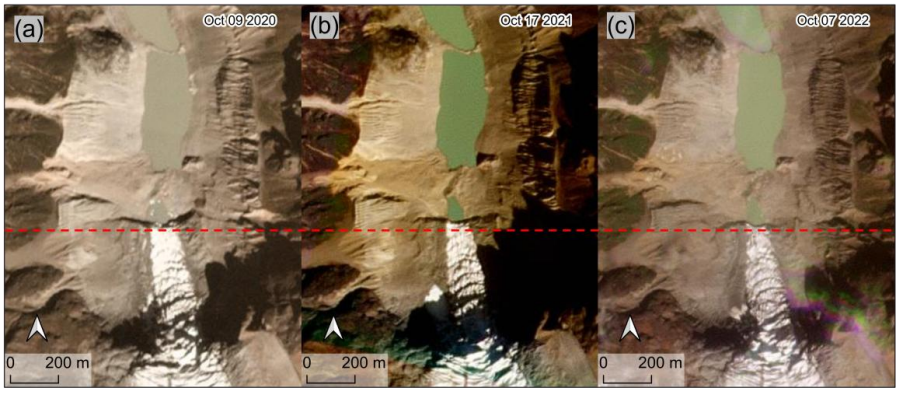

Figure 5 Map of terminus changes of Jinwu Glacier during 2020–2021 based on PlanetScope imagery.

4.3 Surface elevation change

Over the past two decades, Jinwu Glacier has experienced sustained surface lowering (Fig. 6). Based on DEM differencing sampled at 50 m intervals within a 400 m wide swath, the terminal 0–550 m section showed enhanced thinning, with the mean surface elevation change rate changing from −2.90 m a^{-1} during 2002–2014 to −3.71 m a^{-1} during 2014–2025. By contrast, thinning in the upstream 600–1550 m section slowed, with the mean rate changing from −1.17 to −0.87 m a^{-1} over the same periods. A similar spatial pattern is also evident in the dataset of Hugonnet et al. (2021) for 2000–2019 and in that of Brun et al. (2017) for 2000–2016 (Fig. 6). Notably, relatively large discrepancies are found among the different datasets within the terminal 0–550 m section (Fig. 6c), as further discussed in Sect. 5.2.

https://doi.org/10.5194/egusphere-2026-1492
Preprint. Discussion started: 10 April 2026

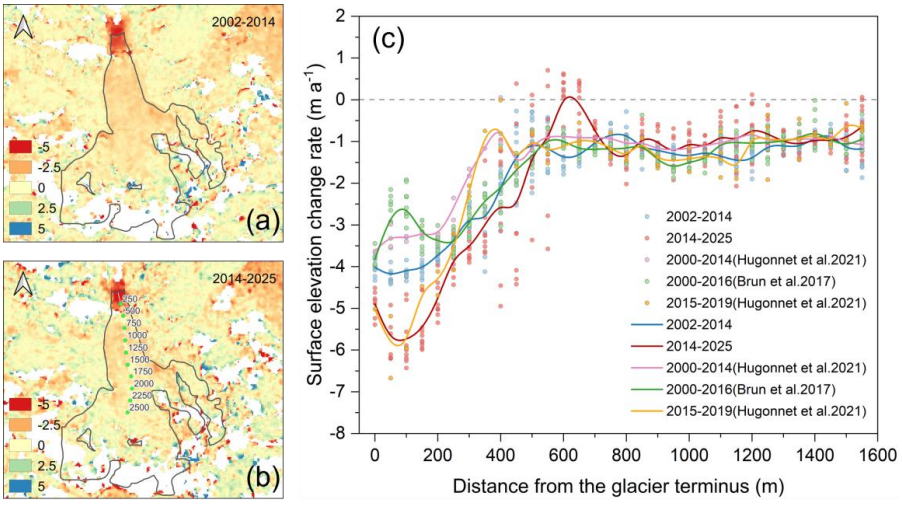

Figure 6 Spatial patterns and longitudinal profiles of surface elevation change rates (dh/dt) of Jinwu Glacier. Maps of dh/dt for the periods 2002–2014 (a) and 2014–2025 (b). (c) shows longitudinal profiles sampled every 50 m along the glacier centerline and averaged within a 400 m-wide swath.

5 Discussion

5.1 Glacier dynamic response to GLOF-induced lake detachment

For Jinwu Glacier, terminus dynamics prior to the GLOF were likely dominated by lake conditions, particularly lake depth (Minowa et al., 2023). Our analysis shows that when lake depth exceeded 10 m (measured after the GLOF) (Zhang et al., 2023a), ice-flow velocity (600-1550m) was significantly positively correlated with lake depth ($p < 0.001$, $R^2 = 0.78$, Fig. S4). Following the 2020 GLOF, the loss of ice–water contact likely increased basal resistance at the glacier terminus, contributing to its subsequent deceleration (Fig. 4a). However, a more pronounced and persistent low-velocity state appeared only after 2022 (Fig. 4c), suggesting that the glacier terminus likely experienced a rapid but short-lived adjustment phase. Lowering of the lake level reduces hydrostatic pressure and buoyant support (Benn et al., 2012). The glacier terminus may therefore have temporarily maintained, or even locally enhanced, extensional flow. As a result, the deceleration signal may have been delayed. This is consistent with geomorphic evidence from both satellite imagery and field observations. PlanetScope imagery indicates marked degradation of the terminus ice cliff after 2021, while the glacier terminus position exhibited a slight advance (Fig. 5). In addition, UAV surveys and field investigations conducted by Peng et al. (2023) in 2021 showed that ice calving occurred at the glacier terminus after the GLOF. A

https://doi.org/10.5194/egusphere-2026-1492
Preprint. Discussion started: 10 April 2026

similar nonlinear response has been reported for other lake-terminating glaciers. For example, Longbasaba Glacier showed above average acceleration in 2006 after engineering works lowered lake level by about 5.6 m in 2005 (Liu et al., 2020). Although surface elevation lowering near the terminus (0-200m) intensified over 2014–2025 (Fig. 6c), the dataset of Hugonnet et al. (2021) indicates that thinning in this sector had already been increasing during 2000–2019 (Fig. S5). Enhanced terminus thinning therefore appears to reflect a longer-term retreat trend, rather than a signal initiated only after the GLOF. Furthermore, poor agreement among elevation change datasets in the 0–550 m zone (Sect. 5.2) limits robust assessment of post-GLOF surface elevation changes near the glacier terminus.

In contrast, surface elevation changes in the upstream sector (600–1550 m) are more reliably (Sect. 5.2) assessed due to better agreement among different datasets (Fig. 6c). Within the 500–750 m reach, our results show that surface lowering slowed from −1.20 m a^{-1} during 2002–2014 to −0.57 m a^{-1} during 2014–2025. Hugonnet et al. (2021) reported a rate of −1.09 m a^{-1} for the same reach during 2015–2019. Taken together, these results suggest that surface lowering in this reach may have slowed further after the GLOF, with a simple time weighted estimate of approximately −0.14 m a^{-1} for 2020–2025. Ice-flow velocity in the upstream 600–1550 m sector decreased after the flood (Fig. 4d), but the magnitude of the reduction (~14%) was smaller than that at the glacier terminus (~49%). As terminus flow slowed, the downstream ice-flux demand imposed on the upstream ice flow likely decreased, favouring the development of compressive flow in the 500-750m section. Additionally, the reduced interannual variability in velocity suggests that, following the disappearance of the proglacial lake, the glacier terminus became more stable. After a short period of dynamic adjustment, glacier changes may have gradually shifted back toward being primarily controlled by climatic forcing.

Proglacial lakes are commonly regarded as a significant non-climatic forcing factor influencing lake-terminating glaciers (Carrivick and Tweed, 2013). In contrast, a GLOF is a sudden perturbation that can rapidly reset glacier terminus boundary conditions by lowering lake level and removing ice–lake contact. The lagged and spatially variable response of Jinwu Glacier further suggests that such events can modify longitudinal coupling, stress transfer, and ice-flux demand between upstream and downstream sections. As moraine-dammed GLOFs become more frequent under ongoing climate warming (Zhang et al., 2025), they should be regarded as event-driven processes in future assessments of lake-terminating glacier dynamics and associated hazards.

https://doi.org/10.5194/egusphere-2026-1492
Preprint. Discussion started: 10 April 2026

5.2 Uncertainty analysis

In this study, uncertainties in surface velocity and elevation change were assessed from residual statistics over stable terrain adjacent to the glacier, thereby quantifying both systematic and random errors. Nevertheless, such estimates do not account for all potential error sources. In the case of surface velocity, image matching can be degraded by repetitive or self-similar glacier surface features, such as crevasses, seracs, and landslide or avalanche deposits, which may increase noise and produce mismatches (Paul et al., 2015). For surface elevation change, additional uncertainties may arise from terrain dependent biases linked to slope (Li and Hajnsek, 2025; Nuth and Kääb, 2011).

A high noise region is observed in the velocity field within 200 to 450 m of the glacier terminus likely because image matching is degraded by an icefall (Fig. 1e) and dense crevassing (Fig. 5). These conditions may reduce the stability of image matching. Moreover, Jinwu Glacier is north facing, and this reach is more frequently affected by topographic shadowing (Fig. S1). Although we prioritized image pairs with minimal shadow influence, residual shadow effects are difficult to fully eliminate. This may further elevate the noise level in this area and could also explain the lower ITS_LIVE velocities observed there (Fig. 4a). To further constrain the accuracy of our velocity estimates, we performed an independent validation based on manual interpretation (Sato et al., 2022; Hyde et al., 2025). We selected 36 clearly identifiable tie points on the image pairs (Fig. S6). The validation shows a root mean square error (RMSE) of 3.61 m a^{-1} between the PlanetScope velocities and the manually derived estimates (Fig. S7).

Surface elevation change estimates from different data sources show relatively poor agreement in the terminus sector (0–550 m, Fig. 6c). The discrepancy with Brun et al. (2017) is mainly expressed in the elevation-change gradient within the 0–200 m zone, whereas that with Hugonnet et al. (2021) is primarily reflected in the thinning magnitude across the 0–550 m sector. Quantitatively, pairwise RMSE values within 0–550 m from 0.75 to 0.97 m a^{-1}, and the mean standard deviation among the three profiles is 0.532 m a^{-1}. By contrast, agreement is substantially improved in the upstream sector (600–1550 m), where RMSE decreases to 0.18–0.29 m a^{-1} and the mean standard deviation drops to 0.162 m a^{-1}. This contrast indicates that surface elevation change estimates are subject to markedly greater uncertainty near the glacier terminus, whereas estimates from the upstream sector are comparatively robust. A likely explanation for this discrepancy is the complex and steep topographic setting of the Jinwu Glacier terminus. DEM elevation errors generally increase with slope (Hugonnet et al., 2022), and residual

https://doi.org/10.5194/egusphere-2026-1492
Preprint. Discussion started: 10 April 2026

horizontal offsets in DEM differencing can be amplified over steep terrain, where they are translated into larger apparent elevation differences (Nuth and Kääb, 2011; Li and Hajnsek, 2025). In addition, the highly crevassed surface, pronounced local shadowing, and complex surface texture of the terminus may degrade DEM extraction, image matching and DEM co-registration quality (Berthier et al., 2014). These effects likely accumulate in the terminus sector and reduce the consistency of elevation-change estimates among datasets. Importantly, although different datasets yield somewhat different thinning magnitudes in the terminus sector, they consistently indicate substantial surface lowering. This suggests that the conclusion of pronounced thinning near the glacier terminus area is robust, even though the exact magnitude of thinning should be interpreted with caution.

6 Conclusion

Using historical remote sensing data, we reconstructed the dynamic evolution of Jinwu Glacier in southeastern Tibet, China, as it transitioned from a lake-terminating to a land-terminating glacier following the glacial lake outburst flood (GLOF) on 26 June 2020. Annual surface velocities were derived from multi-temporal PlanetScope imagery (2017–2025) using feature tracking, and surface elevation changes were quantified from ASTER stereo DEM differencing for the periods 2002–2014 and 2014–2025.

Our results show that the GLOF driven change in glacier terminus boundary conditions triggered a pronounced but lagged dynamic response. Ice-flow velocities within 0–200 m decreased significantly after 2021, with an overall reduction of approximately 49%. In contrast, velocities within 600–1550 m also declined, but the magnitude of change was smaller (approximately 14 %). Surface elevation changes reveal strong spatial contrasts. Thinning within 0–200 m of the terminus intensified after 2014, whereas thinning within 600–1550 m slowed. Notably, a slight surface elevation increase was observed in the topographic transition zone at 500–750 m. In addition, the glacier terminus showed slight advance and local ice calving after the GLOF. Following the loss of proglacial lake influence, the glacier terminus underwent rapid geometric and stress adjustment. Near the terminus, the adjustment likely involved enhanced longitudinal extension. Farther upstream, reduced ice-flow velocity and weakened downstream ice-flux demand may have promoted a shift toward a more compressive strain regime. After this short-

https://doi.org/10.5194/egusphere-2026-1492
Preprint. Discussion started: 10 April 2026

lived dynamic adjustment, subsequent glacier change may have become increasingly governed by climatic forcing.

Overall, our study provides the first quantitative constraints on the glacier response to a GLOF driven reset of terminus boundary conditions, advancing understanding of lake-terminating glacier behaviour and its future evolution under uncertain climate scenarios.

Data availability

The Landsat TM/ETM+/OLI imagery used in this study is publicly available from the U.S. Geological Survey (USGS) archive (https://www.usgs.gov/landsat-missions/landsat-data-access, last access: 24 January 2026). ASTER L1A stereo data are publicly available from the NASA Land Processes Distributed Active Archive Center (LP DAAC; https://www.earthdata.nasa.gov/data/catalog/lpcloud-ast-l1a-004, last access: 11 February 2026). The SRTM DEM is publicly available from the USGS/NASA archive (https://www.usgs.gov/centers/eros/science/usgs-eros-archive-digital-elevation-shuttle-radar-topography-mission-srtm, last access: 3 February 2026). PlanetScope imagery was provided by Planet Labs Inc. through the Education and Research Programme and accessed via Planet Explorer (https://www.planet.com/, last access: 27 January 2026). The Hugonnet et al. (2021) dataset is available at https://www.sedoo.fr/theia-publication-products/?uuid=c428c5b9-df8f-4f86-9b75-e04c778e29b9 (last access: 16 February 2026), and the Brun et al. (2017) dataset is available at https://doi.org/10.1594/PANGAEA.876545 (last access: 29 January 2026). The derived datasets supporting the main findings of this study, including proglacial lake outlines from 1990 to 2025, glacier surface velocity data from 2017 to 2025, and DEMs covering the glacierized area, are openly available at https://doi.org/10.5281/zenodo.19450085 (Luo, 2026).

Author contributions

Y.L. designed the study, developed the methodology, performed the analysis, and wrote the manuscript. Q.L. provided funding, support, and supervision, and contributed to writing and revising the manuscript. Y.F. contributed to data production and analysis, and to writing and revising the manuscript. Xue.L., Y.Y., J.Y., and G.Z. contributed to data production and analysis. Xuy.L. contributed to discussion and manuscript revision. All authors contributed to the final version of the paper.

https://doi.org/10.5194/egusphere-2026-1492
Preprint. Discussion started: 10 April 2026

Competing interests

The contact author has declared that neither they nor their co-authors have any competing interests.

Financial support

This work was financially supported by the National Key Research and Development Program of China (Grant No. 2024YFC3013400), National Science Foundation of China (Grant No. 42361144874), National Natural Science Foundation of China (Grant No. 42501173), the Postdoctoral Fellowship Program of Chinese Postdoctoral Science Foundation (Grant No. GZB20240721).

References

Ahmed, R.: Glacial Lake Outburst Flood (GLOF) Hazard and Risk Management Strategies: A Global Overview, Water Resources Management, 39, 1-16, 10.1007/s11269-024-03958-x, 2025.

Benn, D. I., Hulton, N. R. J., and Mottram, R. H.: 'Calving laws', 'sliding laws' and the stability of tidewater glaciers, Ann Glaciol, 46, 123-130, 10.3189/172756407782871161, 2007.

Benn, D. I., Bolch, T., Hands, K., Gulley, J., Luckman, A., Nicholson, L. I., Quincey, D., Thompson, S., Toumi, R., and Wiseman, S.: Response of debris-covered glaciers in the Mount Everest region to recent warming, and implications for outburst flood hazards, Earth-Science Reviews, 114, 156-174, https://doi.org/10.1016/j.earscirev.2012.03.008, 2012.

Berthier, E., Vincent, C., Magnússon, E., Gunnlaugsson, Á. Þ., Pitte, P., Le Meur, E., Masiokas, M., Ruiz, L., Pálsson, F., Belart, J. M. C., and Wagnon, P.: Glacier topography and elevation changes derived from Pléiades sub-meter stereo images, The Cryosphere, 8, 2275-2291, 10.5194/tc-8-2275-2014, 2014.

Beyer, R. A., Alexandrov, O., and McMichael, S.: The Ames Stereo Pipeline: NASA's Open Source Software for Deriving and Processing Terrain Data, Earth and Space Science, 5, 537-548, https://doi.org/10.1029/2018EA000409, 2018.

Bhattacharya, A., Bolch, T., Mukherjee, K., King, O., Menounos, B., Kapitsa, V., Neckel, N., Yang, W., and Yao, T.: High Mountain Asian glacier response to climate revealed by multi-temporal satellite observations since the 1960s, Nat Commun, 12, 4133, 10.1038/s41467-021-24180-y, 2021.

Brun, F., Berthier, E., Wagnon, P., Kaab, A., and Treichler, D.: A spatially resolved estimate of High Mountain Asia glacier mass balances, 2000-2016, Nat Geosci, 10, 668-673, 10.1038/NGEO2999, 2017.

https://doi.org/10.5194/egusphere-2026-1492
Preprint. Discussion started: 10 April 2026

367 Carrivick, J. L. and Tweed, F. S.: Proglacial lakes: character, behaviour and geological importance,
368 Quaternary Sci Rev, 78, 34-52, 10.1016/j.quascirev.2013.07.028, 2013.
369 Gao, Y., Wang, J., Liu, S., Qi, M., Liang, P., and Mu, J.: Mechanisms of glacier surges in the Central
370 Himalayas uncovered using remote sensing and glacier modelling, Geomorphology, 482, 109816,
371 https://doi.org/10.1016/j.geomorph.2025.109816, 2025.
372 Gardner, A. S., Greene, C. A., Kennedy, J. H., Fahnestock, M. A., Liukis, M., López, L. A., Lei, Y.,
373 Scambos, T. A., and Dehecq, A.: ITS_LIVE global glacier velocity data in near-real time, The
374 Cryosphere, 19, 3517-3533, 10.5194/tc-19-3517-2025, 2025.
375 Hanshaw, M. N. and Bookhagen, B.: Glacial areas, lake areas, and snow lines from 1975 to 2012: status
376 of the Cordillera Vilcanota, including the Quelccaya Ice Cap, northern central Andes, Peru, The
377 Cryosphere, 8, 359-376, 10.5194/tc-8-359-2014, 2014.
378 Hugonnet, R., Brun, F., Berthier, E., Dehecq, A., Mannerfelt, E. S., Eckert, N., and Farinotti, D.:
379 Uncertainty Analysis of Digital Elevation Models by Spatial Inference From Stable Terrain, Ieee J-Stars,
380 15, 6456-6472, 10.1109/JSTARS.2022.3188922, 2022.
381 Hugonnet, R., McNabb, R., Berthier, E., Menounos, B., Nuth, C., Girod, L., Farinotti, D., Huss, M.,
382 Dussaillant, I., Brun, F., and Kaab, A.: Accelerated global glacier mass loss in the early twenty-first
383 century, Nature, 592, 726-731, 10.1038/s41586-021-03436-z, 2021.
384 Hyde, A., Carr, R., Dunning, S. A., and Van Wyk de Vries, M.: Quantifying heterogeneous glacier
385 dynamics in Lunana, Bhutan, using spatiotemporally high-resolution satellite imagery, Journal of
386 Glaciology, 71, e126, 10.1017/jog.2025.10103, 2025.
387 Ke, L., Song, C., Yong, B., Lei, Y., and Ding, X.: Which heterogeneous glacier melting patterns can be
388 robustly observed from space? A multi-scale assessment in southeastern Tibetan Plateau, Remote Sens
389 Environ, 242, 10.1016/j.rse.2020.111777, 2020.
390 King, O., Dehecq, A., Quincey, D., and Carrivick, J.: Contrasting geometric and dynamic evolution of
391 lake and land-terminating glaciers in the central Himalaya, Global Planet Change, 167, 46-60,
392 10.1016/j.gloplacha.2018.05.006, 2018.
393 Kitoh, A.: The Asian Monsoon and its Future Change in Climate Models: A Review, Journal of the
394 Meteorological Society of Japan. Ser. II, 95, 7-33, 10.2151/jmsj.2017-002, 2017.

https://doi.org/10.5194/egusphere-2026-1492
Preprint. Discussion started: 10 April 2026

395 Lehner, B. and Grill, G.: Global river hydrography and network routing: baseline data and new
396 approaches to study the world's large river systems, Hydrological Processes, 27, 2171-2186,
397 https://doi.org/10.1002/hyp.9740, 2013.
398 Leprince, S., Barbot, S., Ayoub, F., and Avouac, J. P.: Automatic and precise orthorectification,
399 coregistration, and subpixel correlation of satellite images, application to ground deformation
400 measurements, Ieee T Geosci Remote, 45, 1529-1558, 10.1109/Tgrs.2006.888937, 2007.
401 Li, G., Lv, M., Quincey, D. J., Taylor, L. S., Li, X., Yan, S., Sun, Y., and Guo, H.: Characterizing the
402 surge behaviour and associated ice-dammed lake evolution of the Kyagar Glacier in the Karakoram, The
403 Cryosphere, 17, 2891-2907, 10.5194/tc-17-2891-2023, 2023.
404 Li, S. and Hajnsek, I.: Geodetic glacier mass balance in the Karakoram (2011–2019) from TanDEM-X:
405 An InSAR DEM differencing framework, Remote Sens Environ, 331, 115023,
406 https://doi.org/10.1016/j.rse.2025.115023, 2025.
407 Liu, Q., Mayer, C., Wang, X., Nie, Y., Wu, K., Wei, J., and Liu, S.: Interannual flow dynamics driven
408 by frontal retreat of a lake-terminating glacier in the Chinese Central Himalaya, Earth Planet Sc Lett,
409 546, 10.1016/j.epsl.2020.116450, 2020.
410 Luo, Y.: The 2020 abrupt drainage of Jinwuco triggered lake- to land- terminus transition and lagged
411 slowdown of Jinwu Glacier, southeastern Tibet, Zenodo [dataset],
412 https://doi.org/10.5281/zenodo.19450085, 2026.
413 Luo, Y., Yin, Y., Zhong, Y., Lu, X., Yang, J., Sapkota, L., Lu, X., and Liu, Q.: Dynamics of lake–
414 terminating glaciers in the Himalaya and Southeastern Tibet between 1990 and 2020, Journal of
415 Glaciology, 1-20, 10.1017/jog.2025.10088, 2025.
416 Lützow, N., Veh, G., and Korup, O.: A global database of historic glacier lake outburst floods, Earth
417 System Science Data, 15, 2983-3000, 10.5194/essd-15-2983-2023, 2023.
418 Mattea, E., Berthier, E., Dehecq, A., Bolch, T., Bhattacharya, A., Ghuffar, S., Barandun, M., and Hoelzle,
419 M.: Five decades of Abramov glacier dynamics reconstructed with multi-sensor optical remote sensing,
420 The Cryosphere, 19, 219-247, 10.5194/tc-19-219-2025, 2025.
421 Maurer, J. M., Schaefer, J. M., Rupper, S., and Corley, A.: Acceleration of ice loss across the Himalayas
422 over the past 40 years, Science Advances, 5, eaav7266, doi:10.1126/sciadv.aav7266, 2019.
423 Minowa, M., Schaefer, M., and Skvarca, P.: Effects of topography on dynamics and mass loss of lake-
424 terminating glaciers in southern Patagonia, Journal of Glaciology, 1-18, 10.1017/jog.2023.42, 2023.

https://doi.org/10.5194/egusphere-2026-1492
Preprint. Discussion started: 10 April 2026

425 Nuth, C. and Kääb, A.: Co-registration and bias corrections of satellite elevation data sets for quantifying
426 glacier thickness change, The Cryosphere, 5, 271-290, 10.5194/tc-5-271-2011, 2011.
427 Paul, F., Piermattei, L., Treichler, D., Gilbert, L., Girod, L., Kääb, A., Libert, L., Nagler, T., Strozzi, T.,
428 and Wuite, J.: Three different glacier surges at a spot: what satellites observe and what not, The
429 Cryosphere, 16, 2505-2526, 10.5194/tc-16-2505-2022, 2022.
430 Paul, F., Bolch, T., Kääb, A., Nagler, T., Nuth, C., Scharrer, K., Shepherd, A., Strozzi, T., Ticconi, F.,
431 Bhambri, R., Berthier, E., Bevan, S., Gourmelen, N., Heid, T., Jeong, S., Kunz, M., Lauknes, T. R.,
432 Luckman, A., Merryman Boncori, J. P., Moholdt, G., Muir, A., Neelmeijer, J., Rankl, M., VanLooy, J.,
433 and Van Niel, T.: The glaciers climate change initiative: Methods for creating glacier area, elevation
434 change and velocity products, Remote Sens Environ, 162, 408-426,
435 https://doi.org/10.1016/j.rse.2013.07.043, 2015.
436 Peng, M., Wang, X., Zhang, G., Veh, G., Sattar, A., Chen, W., and Allen, S.: Cascading hazards from
437 two recent glacial lake outburst floods in the Nyainqêntanglha range, Tibetan Plateau, Journal of
438 Hydrology, 626, 10.1016/j.jhydrol.2023.130155, 2023.
439 Pronk, J. B., Bolch, T., King, O., Wouters, B., and Benn, D. I.: Contrasting surface velocities between
440 lake- and land-terminating glaciers in the Himalayan region, The Cryosphere, 15, 5577-5599, 10.5194/tc-
441 15-5577-2021, 2021.
442 Richardson, S. D. and Reynolds, J. M.: An overview of glacial hazards in the Himalayas, Quaternary
443 International, 65-66, 31-47, https://doi.org/10.1016/S1040-6182(99)00035-X, 2000.
444 Salerno, F., Thakuri, S., D'Agata, C., Smiraglia, C., Manfredi, E. C., Viviano, G., and Tartari, G.: Glacial
445 lake distribution in the Mount Everest region: Uncertainty of measurement and conditions of formation,
446 Global Planet Change, 92-93, 30-39, 10.1016/j.gloplacha.2012.04.001, 2012.
447 Sanjay, J., Krishnan, R., Shrestha, A. B., Rajbhandari, R., and Ren, G.-Y.: Downscaled climate change
448 projections for the Hindu Kush Himalayan region using CORDEX South Asia regional climate models,
449 Advances in Climate Change Research, 8, 185-198, https://doi.org/10.1016/j.accre.2017.08.003, 2017.
450 Sato, Y., Fujita, K., Inoue, H., and Sakai, A.: Land- to lake-terminating transition triggers dynamic
451 thinning of a Bhutanese glacier, The Cryosphere, 16, 2643-2654, 10.5194/tc-16-2643-2022, 2022.
452 Schomacker, A.: Expansion of ice-marginal lakes at the Vatnajökull ice cap, Iceland, from 1999 to 2009,
453 Geomorphology, 119, 232-236, https://doi.org/10.1016/j.geomorph.2010.03.022, 2010.

https://doi.org/10.5194/egusphere-2026-1492
Preprint. Discussion started: 10 April 2026

454 Shugar, D. H., Burr, A., Haritashya, U. K., Kargel, J. S., Watson, C. S., Kennedy, M. C., Bevington, A.
455 R., Betts, R. A., Harrison, S., and Strattman, K.: Rapid worldwide growth of glacial lakes since 1990,
456 Nat Clim Change, 10, 939-945, 10.1038/s41558-020-0855-4, 2020.
457 Singh Jasrotia, A., Ahmad, S., Ridwan, Q., Ahmad Wani, Z., Siddiqui, S., Siddiqua, A., and Ali Morfeine
458 aika, E.: Estimation of Surface Ice Velocity of Durung Drung Glacier, Western Himalaya using COSI-
459 Corr from Landsat images, The Egyptian Journal of Remote Sensing and Space Sciences, 27, 369-381,
460 https://doi.org/10.1016/j.ejrs.2024.04.006, 2024.
461 Tsutaki, S., Fujita, K., Nuimura, T., Sakai, A., Sugiyama, S., Komori, J., and Tshering, P.: Contrasting
462 thinning patterns between lake- and land-terminating glaciers in the Bhutanese Himalaya, The
463 Cryosphere, 13, 2733-2750, 10.5194/tc-13-2733-2019, 2019.
464 Wang, X., Guo, X., Yang, C., Liu, Q., Wei, J., Zhang, Y., Liu, S., Zhang, Y., Jiang, Z., and Tang, Z.:
465 Glacial lake inventory of high-mountain Asia in 1990 and 2018 derived from Landsat images, Earth
466 System Science Data, 12, 2169-2182, 10.5194/essd-12-2169-2020, 2020.
467 Watson, C. S., Kargel, J. S., Shugar, D. H., Haritashya, U. K., Schiassi, E., and Furfaro, R.: Mass Loss
468 From Calving in Himalayan Proglacial Lakes, Front Earth Sc-Switz, 7, 10.3389/feart.2019.00342, 2020.
469 Yao, T., Thompson, L., Yang, W., Yu, W., Gao, Y., Guo, X., Yang, X., Duan, K., Zhao, H., Xu, B., Pu,
470 J., Lu, A., Xiang, Y., Kattel, D. B., and Joswiak, D.: Different glacier status with atmospheric circulations
471 in Tibetan Plateau and surroundings, Nat Clim Change, 2, 663-667, 10.1038/nclimate1580, 2012.
472 Zemp, M., Jakob, L., Dussaillant, I., Nussbaumer, S. U., Gourmelen, N., Dubber, S., A, G., Abdullahi,
473 S., Andreassen, L. M., Berthier, E., Bhattacharya, A., Blazquez, A., Boehm Vock, L. F., Bolch, T., Box,
474 J., Braun, M. H., Brun, F., Cicero, E., Colgan, W., Eckert, N., Farinotti, D., Florentine, C., Floricioiu, D.,
475 Gardner, A., Harig, C., Hassan, J., Hugonnet, R., Huss, M., Jóhannesson, T., Liang, C.-C. A., Ke, C.-Q.,
476 Khan, S. A., King, O., Kneib, M., Krieger, L., Maussion, F., Mattea, E., McNabb, R., Menounos, B.,
477 Miles, E., Moholdt, G., Nilsson, J., Pálsson, F., Pfeffer, J., Piermattei, L., Plummer, S., Richter, A.,
478 Sasgen, I., Schuster, L., Seehaus, T., Shen, X., Sommer, C., Sutterley, T., Treichler, D., Velicogna, I.,
479 Wouters, B., Zekollari, H., Zheng, W., and The Gla, M. T.: Community estimate of global glacier mass
480 changes from 2000 to 2023, Nature, 639, 382-388, 10.1038/s41586-024-08545-z, 2025.
481 Zhang, G., Bolch, T., Yao, T., Rounce, D. R., Chen, W., Veh, G., King, O., Allen, S. K., Wang, M., and
482 Wang, W.: Underestimated mass loss from lake-terminating glaciers in the greater Himalaya, Nat Geosci,
483 16, 333-338, 10.1038/s41561-023-01150-1, 2023a.

https://doi.org/10.5194/egusphere-2026-1492
Preprint. Discussion started: 10 April 2026

Zhang, T., Wang, W., and An, B.: Heterogeneous changes in global glacial lakes under coupled climate warming and glacier thinning, Communications Earth & Environment, 5, 374, 10.1038/s43247-024-01544-y, 2024.

Zhang, T., Wang, W., An, B., and Wei, L.: Enhanced glacial lake activity threatens numerous communities and infrastructure in the Third Pole, Nature Communications, 14, 8250, 10.1038/s41467-023-44123-z, 2023b.

Zhang, T., Wang, W., Kougkoulos, I., Cook, S. J., Li, S., Iribarren-Anacona, P., Watson, C. S., An, B., and Yao, T.: High frequency of moraine-dammed lake outburst floods driven by global warming, Nature Communications, 16, 11173, 10.1038/s41467-025-67650-3, 2025.

Zheng, G., Bao, A., Allen, S., Antonio Ballesteros-Cánovas, J., Yuan, Y., Jiapaer, G., and Stoffel, M.: Numerous unreported glacial lake outburst floods in the Third Pole revealed by high-resolution satellite data and geomorphological evidence, Science Bulletin, 66, 1270-1273, 10.1016/j.scib.2021.01.014, 2021a.

Zheng, G., Mergili, M., Emmer, A., Allen, S., Bao, A., Guo, H., and Stoffel, M.: The 2020 glacial lake outburst flood at Jinwuco, Tibet: causes, impacts, and implications for hazard and risk assessment, The Cryosphere, 15, 3159-3180, 10.5194/tc-15-3159-2021, 2021b.

Zheng, G., Allen, S. K., Bao, A., Ballesteros-Cánovas, J. A., Huss, M., Zhang, G., Li, J., Yuan, Y., Jiang, L., Yu, T., Chen, W., and Stoffel, M.: Increasing risk of glacial lake outburst floods from future Third Pole deglaciation, Nat Clim Change, 11, 411-417, 10.1038/s41558-021-01028-3, 2021c.